The American Journal of Pathology, Vol. 175, No. 4, October 2009

DOI: 10.2353/ajpath.2009.080845

Cardiovascular, Pulmonary and Renal Pathology

Nitric Oxide Induces the Progression of Abdominal Aortic Aneurysms through the Matrix Metalloproteinase Inducer EMMPRIN

Tania R. Lizarbe,* Carlos Tarín,* Mónica Gómez,* Begoña Lavin,* Enrique Aracil,† Luis M. Orte,† and Carlos Zaragoza*

From the Institutional Fundación Centro Nacional de Investigaciones Cardiovasculares, Madrid; and Hospital Universitario Ramón y Cajal,† Madrid, Spain*

Nitric Oxide (NO) is involved in the development and progression of abdominal aortic aneurysms (AAA). We found that inhibition of inducible NO synthase (iNOS) protects mice in an elastase-induced AAA model, significantly inhibiting the production of matrix metalloproteinase-13 (MMP-13). The extracellular MMP inducer (EMMPRIN; CD147) was increased in human AAA biopsies and in wild-type murine AAA but not in AAA from iNOS null mice. In cells overexpressing ectopic EMMPRIN, MMP-13 secretion was stimulated, whereas silencing of EMMPRIN by RNA interference led to significant inhibition of MMP-13 expression. In addition, elastase infusion of MMP-13 null mouse aortas induced a significant increase of EMMPRIN but reduced aortic dilatation when compared with wild-type mice, suggesting that NO-mediated AAA may be mediated through EMMPRIN induction of MMP-13. These findings were further verified in elastase-infused iNOS null mice, in which daily administration of NO caused a significant aortic dilatation and the expression of EMMPRIN and MMP-13. By contrast, in iNOS wild-type mice, pharmacological inhibition of iNOS by administration of 1400 W induced a reduction of aortic diameter and inhibition of MMP-13 and EMMPRIN expression when compared with control mice. Our results suggest that NO may regulate the development of AAA in part by inducing the expression of EMMPRIN and modulating the activity of MMP-13 in murine and human aneurysms. ***(Am J Pathol 2009, 175:1421–1430; DOI: 10.2353/ajpath.2009.080845)***

Abdominal aortic aneurysm (AAA) is an age-related multifactorial cardiovascular disease and is usually asymptomatic until rupture or diameter size requires medical intervention.[1,2]

AAA is characterized by local chronic inflammation, degradation of the medial elastin, and components of the extracellular matrix. Resistance to rupture depends on tensile strength by interstitial collagens, and therefore, collagen-degrading enzymes may play a pivotal effect.[3]

Matrix metalloproteinases (MMPs) are extracellular matrix degrading enzymes involved in the development and progression of AAA in humans and mice. The effect of collagenases MMP-8[3] and MMP-13,[4] gelatinases A and B,[5] and membrane type MMPs[6] have been extensively analyzed. In particular, collagenases are responsible of cleavage of type I and III collagens, which are involved in keeping the vessel tensile strength, and therefore, increased production of collagen-degrading enzymes may be determinant for the progression of AAA. However, the molecular mechanisms leading to MMP expression and activation are not fully understood.

The expression of MMPs have been recently associated to cardiovascular disease through the activation of the extracellular MMP inducer (EMMPRIN; Basigin and CD147).[7] EMMPRIN is an immunoglobulin, which induces the expression of MMP-2, MMP-9, and MT1-MMP.[8–13] Acute and chronic inflammation induces the expression of EMMPRIN by immune cells and vascular endothelial cells, and its role on MMP expression was related to atherosclerosis.[14,15]

Here we show the association of EMMPRIN and MMP-13 in human AAA and during the NO-mediated AAA in mice, providing evidence about the effect of EMMPRIN on MMP-13 expression in vascular cells.

Supported by the Ministerio de Educación y Ciencia, Plan Nacional de I+D+I (SAF 2005-06025; to C.Z.).

T.R.L. and C.T. contributed equally.

Accepted for publication June 30, 2009.

Supplemental material for this article can be found on *http://ajp.amjpathol.org.*

Address reprint requests to Carlos Zaragoza, Centro Nacional de Investigaciones Cardiovasculares, Melchor Fernández Almagro 3, 28029 Madrid, Spain. E-mail: czaragoza@cnic.es.

Materials and Methods

Reagents

General cell culture supplies were from BD Biosciences (Spain), calf serum was from BioWhittaker (Verviers, Belgium), and cell culture gelatin, antibiotics, and trichrome staining (Masson) was from Sigma-Aldrich (St. Louis, MO). Autoradiography film was from Kodak; polyvinylidene difluoride protein transfer membranes were from Millipore (Iberica, Spain); and horseradish peroxidase-conjugated secondary antibodies and the enhanced chemiluminescence immunoblot detection system were from GE HealthCare (Spain). EDTA-free protease inhibitor mixture tablets were from Roche (Spain). Optimem and Lipofectamine were from Invitrogen. Fluorsave coverslip mounting solution was from Calbiochem (CN Biosciences, UK). EMMPRIN small interfering RNAs were from Qiagen (Qiagen Iberia, Spain). Porcine elastase (specific activity 5 U/mg; E1250) was from Sigma-Aldrich. Primary antibodies were obtained as follows: rabbit anti-MMP-13 from Calbiochem; goat-anti-human-MMP-13 and rabbit anti-inducible NO synthase (iNOS) from Santa Cruz Biotechnology (Santa Cruz, CA); rabbit anti-MMP-2, mouse anti-MMP-9, rabbit anti-MMP-12, and mouse anti-glyceraldehyde-3-phosphate dehydrogenase (GAPDH) from Chemicon (Millipore, Iberica, Spain); anti-FLAG, and goat-anti-EMMPRIN from Sigma-Aldrich; anti-ICAM-2, anti-von Willebrand factor, and anti-Mac-3 from Transduction Laboratories (BD Biosciences). Rat-anti-mouse polymorphonuclear from Serotec (Oxford, UK). Mouse-anti-human EMMPRIN was donated by Prof. Francisco Sánchez (Centro Nacional de Investigaciones Cardiovasculares, Madrid, Spain).

Animals

The institutional ethics committee previously approved, and written consent was obtained for the animal procedures performed in this work. Wild-type C57BL/6 mice, C57BL/6 iNOS null mice, and C57BL/6 apoE null mice were purchased from The Jackson Laboratory (Bar Harbor, ME). C57BL/6 MMP-13 null mice were donated by Dr. Stephen Krane (Department of Medicine, Harvard Medical School, Boston, MA). All animals were housed in our animal facilities in isolated rooms. AAA experiments were performed in 45- to 50-week-old mice, with the exception of experiments conducted to determine changes in aortic diameter (AD), in which 12-week-old mice were used for this purpose. Atherosclerosis was induced in mice fed with Western type diet for 16 weeks (42% fat, Harland Teklad, TD88137).

Human Tissue Samples

Institutional ethics committee approval for the study was obtained, and written consent was granted from all patients. Tissue from 18 patients under surgery was obtained intraoperatively from the anterior aneurysm wall. Biopsies were embedded in paraffin for immunohistochemistry purposes. Morphometric analysis of AAA was evaluated by preoperative computed tomography. Additional information of patients was recorded and summarized in Supplemental Table 1 (see *http://ajp.amjpathol.org*). In addition, ascending aortic tissue was collected from non-AAA-diagnosed patients subjected to coronary intervention for control purposes.

Cells

Murine aortic endothelial cells were grown on gelatin as described previously.[16]

Elastase Infusion of Mice

Mice (12 and 45 to 50 weeks) were anesthesized by i.p. injection of ketamine (100 mg/kg)/xylazine (5 mg/kg), and a horizontal laparatomy was practiced. With a surgical stereomicroscope (Nikon), the abdominal aorta was isolated. Below the renal arteries and above iliac arteries, the abdominal aorta was temporary ligated, and an aortotomy was created with a 30-gauge needle. A PE-26 polyetilene tube was introduced through the aortotomy, and the aorta was infused at 100 mmHg, either with saline buffer or with type I porcine pancreatic elastase (0.4 U/ml), for 5 minutes. The aortotomy was then repaired, ligation was eliminated, and blood flow restoration was visualized. Elastase-infused mice and sham operated (saline-infused) controls were closed, housed, and subjected to further experimentation.

Photographs of abdominal aortas were recorded before infusion, right after infusion, 15 days postinfusion, and 21 days postinfusion, and ADs were measured.

Plasmids and Cell Transfection

Epitope-tagged constructs encoding full-length EMMPRIN were expressed in endothelial cells. The cDNA encoding recombinant protein was cloned in p3XFLAG-myc-CMV-24 (Sigma-Aldrich), which tags expressed proteins with FLAG and myc epitopes at the N-terminus and the C-terminus, respectively. For exogenous EMMPRIN expression and gene and silencing, cells were transiently transfected using Lipofectamine 2000 Reagent as described previously.[16]

In Vivo *Nuclear Magnetic Resonance and Angiography*

Mice were anesthesized with 4% isoflurane/O_2 gas and maintained with 1.5% isoflurane/O_2 gas. A respiration triggering probe was connected to a triggering unit, and images were acquired on a Bruker Biospec BMT 47/40 spectrometer (Bruker, Ettlingen, Germany) 4.7 T, equipped with 11.2 cm actively shielded gradient system, capable of 200 mT/m gradient strength and 80-seconds rise time. Global shimming was first performed, and three scout images in axial, sagittal, and coronal direction were acquired using a T1 weighted spin echo sequence (repetition time/echo time = 200/10 ms). Then, respiratory-gated T1-weighted spin echo images in sag-

ittal orientation were acquired. Repetition time varied from 500 to 700 ms, depending on the respiratory rate of each animal, and echo time was 15 ms. Fifteen sagittal slices of 1.0 mm were acquired with an in-plane field of view (FOV) of 4 × 2 cm^2 and matrix size of 256 × 128. Respiratory-gated T1-weighted spin-echo axial images were acquired using the same parameters as above, with a FOV of 3 × 3 cm^2 and a matrix of 256 × 192. Twenty-four slices were acquired, and data were zero filled to obtain images of 256 × 256 pixels. For the magnetic resonance angiography, a gradient echo with flow compensation imaging sequence was used with the following parameters: repetition time = 45 ms; echo time = 10 ms; flip angle = 80°; acquisition matrix size = 256 × 128; FOV = 3.5 × 1.75 cm^2; and number of slices: 64, 0.5 mm/slice. Slices were overlapped 0.1 mm, with a FOV in the slice direction of 2.57 cm.

Maximal AD was determined between the renal and the iliac arteries with the ParaVision software package (Bruker). Data set was first interpolated to obtain isotropic voxels of 137 × 137 × 137_m^3. The acquired matrix was of 256 × 128 × 64, covering a FOV of 3.5 × 1.75 × 2.57 cm^3. The resulting matrix was interpolated to a 256 × 128 × 128 matrix. Maximum Intensity Projection algorithm was applied to the interpolated data to obtain a three-dimensional view of each angiography.

Immunoblotting

Cell lysis and immunoblotting were performed as described previously.[16]

Confocal Microscopy

Proteins were detected by confocal microscopy in cultured cells and paraffin-embedded tissue sections. Cell cultures were grown on coverslips and, after treatment, were washed twice with PBS. Cells were fixed for 10 minutes with cold methanol and incubated for 1 hour with 3% bovine serum albumin in PBS. Coverslips were then washed with PBS and incubated with the appropriate primary antibodies for 1 hour. Nonbound antibody was removed by washing four times with PBS, after which coverslips were incubated with an appropriate fluorescence-conjugated secondary antibody for 1 hour. Staining was visualized by confocal microscopy (Radiance 2100; Bio-Rad, Hercules, CA). Proteins were detected with secondary antibodies tagged with the flurochromes Cy3 or fluorescein isothiocyanate. Cell nuclei were stained with Hoechst.

Immunohistochemistry

Paraffin-embedded tissue from mice and human biopsies were sliced 4 μm thick. Elastin integrity of mouse aortas was monitored by Trichrome staining and visualized by light microscopy. In human biopsies, iNOS, EMMPRIN, and MMP-13 were visualized as follows: sections were incubated with normal serum in PBS, washed 5 minutes with PBS, and then incubated for 1 hour with the corresponding primary antibody in humidified chambers. Controls were also incubated with nonimmune serum. Slices were washed three times with PBS and then incubated with horseradish peroxidase-conjugated secondary antibodies. Immunoreactive complexes were detected with alkaline phosphatase substrate. Before visualization, sections were also stained with hematoxylin.

Statistical Analysis

Unless otherwise specified, data are expressed as means ± SD, and experiments were performed at least three times in duplicate. Whenever comparisons were made with a common control, comparisons were made with analysis of variance followed by Dunnett's modification of the *t*-test. The level of statistical significance was defined as $P < 0.05$. Error bars represent ±SD.

Results

Lack of iNOS Inhibits the Progression of AAA in Mice

We induced AAA in mice by the infusion of porcine elastase in the infra-renal abdominal aorta and compared the variation of AD over time respect to saline-infused sham operated animals, as described previously.[17] Changes in aortic diameter were evaluated in 12-week-old and 40- to 50-week-old wild-type mice (C57BL/6), iNOS null mice, apoE null mice, and iNOS/apoE null mice, either infused with elastase or saline as described. As shown in Table 1, we found no differences in AD in 12-week-old mice over time. However, in older animals, we found extensive aortic dilatation 14 days after elastase infusion in wild-type mice respect to mice lacking iNOS (iNOS null mice and iNOS/apoE null mice), in association with destruction of aortic lamellae, as detected by Masson Trichromic (Figure 1A) and by Verhoeff-van Gieson staining of aortic sections (Supplemental Figure S1, see *http://ajp.amjpathol.org*), and significant increase of iNOS expression (Figure 1B). No significant differences were detected in 40- to 50-week-old sham operated mice in AD (Table 1) and immune cell infiltration in response to NO (Supplemental Figure S1B, see *http://ajp.amjpathol.org*). The progression of AAA was also followed by magnetic resonance imaging over time with similar results (Figure 1C; Supplemental Figures S1C and S1D, see *http://ajp.amjpathol.org*).

To evaluate the effect of NO in the progression of AAA in atherosclerotic mice, we generated iNOS/apoE double-knockout animals and fed them with high cholesterol diet (see *Materials and Methods* for details). We found that after elastase infusion, no significant variations on aortic dilatation were detected in double iNOS/apoE null mice when compared with single apoE knockouts (Figure 1 and Table 1; Supplemental Figures S1C and S1D, see *http://ajp.amjpathol.org*).

Table 1. Changes in AD Over Time

Strain	AD prior	AD after	AD 14 days
Elastase-infused mice (12-week-old mice)			
C57BL/6	0.5 ± 0.02	0.77 ± 0.03	1.3 ± 0.2
apoE null	0.5 ± 0.2	0.78 ± 0.03	1.4 ± 0.5
iNOS null	0.5 ± 0.01	0.75 ± 0.01	1.2 ± 0.2
apoE/iNOS null	0.5 ± 0.2	0.78 ± 0.0.4	1.3 ± 0.02
Elastase-infused mice (40- to 50-week-old mice)			
C57BL/6	0.5 ± 0.01	0.75 ± 0.02	1.8 ± 0.04
apoE null	0.5 ± 0.12	0.79 ± 0.03	1.9 ± 0.04
iNOS null	0.5 ± 0.01	0.77 ± 0.01	1.02 ± 0.03
apoE/iNOS null	0.5 ± 0.2	0.82 ± 0.025	0.92 ± 0.02
Sham-operated mice (40- to 50-week-old mice)			
C57BL/6	0.5 ± 0.02	0.76 ± 0.02	0.8 ± 0.04
apoE null	0.5 ± 0.02	0.77 ± 0.02	0.8 ± 0.04
iNOS null	0.5 ± 0.01	0.77 ± 0.01	0.9 ± 0.03
apoE/iNOS null	0.5 ± 0.2	0.79 ± 0.02	0.8 ± 0.02

AD, aortic diameter; prior, prior infusion; after, after infusion; 14 days, 14 days after infusion. $N = 10$ animals/strain/, repeated three times.

Lack of iNOS Inhibits the Expression of MMP-13 in Murine AAA

The expression of MMPs is associated to AAA in mice and in humans. In this regard, we evaluated the aortic expression of MMP-2, MMP-9, MMP-12, and MMP-13 during the course of AAA in iNOS wild-type and iNOS null mice, finding increased expression of MMP-2, MMP-9, and MMP-12 over time in both groups (Supplemental Figures S2 and S3, see *http://ajp.amjpathol.org*), with the exception of MMP-13, whose expression was significantly reduced in iNOS null mice 15 days after elastase infusion, when compared with wild-type mice, as detected by immunofluorescence (Figure 2A) and immunoblot (Figure 2B), suggesting a role for MMP-13 in the NO-mediated effect on AAA. In view of this result, and taking into account that MMP-13 is associated to human AAA,[3] that NO up-regulates the expression of MMP-13 *in vivo*[16,18,19] and that NO and MMP-13 are associated in atherosclerosis,[20] we decided to evaluate the association between NO an MMP-13 at the molecular level during the course of AAA.

Expression of EMMPRIN Is Inhibited in iNOS Null Mice

Recently, the expression of EMMPRIN was found associated to different cardiovascular diseases, including ath-

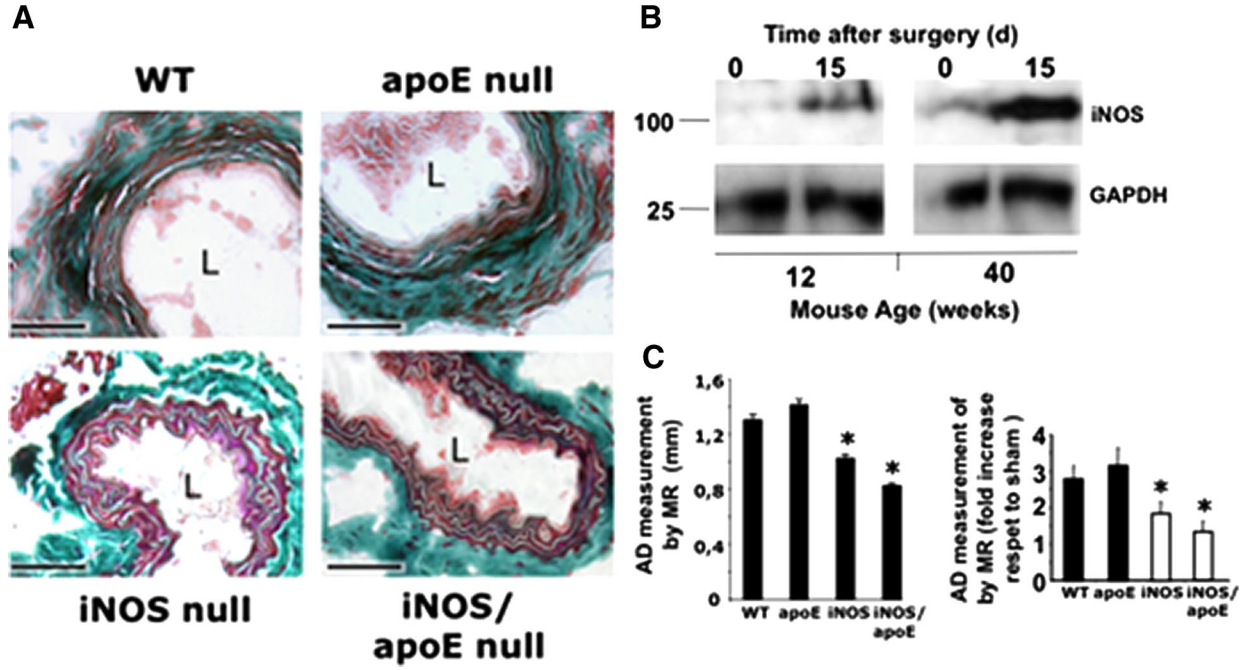

Figure 1. Lack of iNOS protects mice during induction of AAA. **A:** Thrichrome Masson staining of aortic sections from C57BL/6 wild-type mice (WT), iNOS null mice, apoE null mice and iNOS/apoE double null mice, 15 days after surgery. Scale bars, 100 μm ($n = 6$). **B:** Immunoblot detection of iNOS in 12- and 40-week-old mice aortic lysates, 15 days after elastase infusion. **C:** Effect of NO on aortic dilatation overtime. Ten animals per group were either infused with elastase or saline buffer, and the aortas were monitored over time by magnetic resonance. **Left**, Graphical representation of AD 15 days after elastase infusion. **Right**, Graphical representation of the increase in diameter 15 days after surgery respect to sham operated mice ($n = 10$mice/genotype/assay by triplicate mean ± SD; $^*P < 0.05$ vs wild-type). L, lumen.

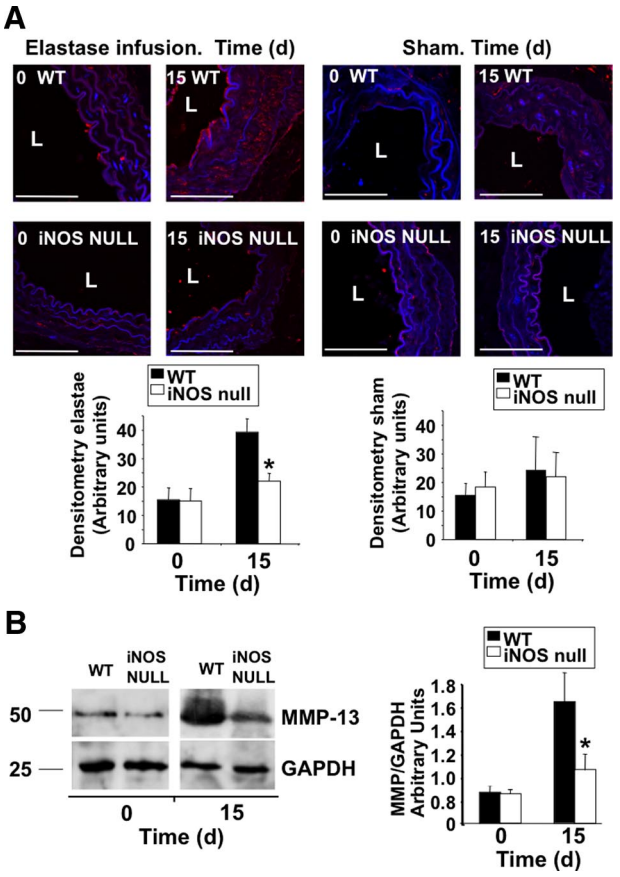

Figure 2. Lack of iNOS inhibits the expression of MMP-13 in AAA. **A:** Immunofluorescence detection of MMP-13 in aortic ring sections from wild-type (WT) and iNOS null mice, collected after elastase infusion (**left panels**), or saline infusion (**right panels**) over time ($n = 3$ mice/time point by triplicate, mean ± SD; $^{*}P < 0.05$ vs wild-type) L: lumen. Scale bars, 50 μm. **B:** Immunoblot detection of MMP-13 in the same mice as in **A**. GAPDH was also detected for control loading purposes. **Right**, Densitometric analysis of the immunoreactive bands detected at time points 0 and 15 days after surgery ($n = 3$ mice/time point by triplicate, mean ± SD; $^{*}P < 0.05$ vs wild type).

erosclerosis and myocardial infarction.[7,15,21–24] Here we found EMMPRIN accumulation at the endothelial layer of aortas in which AAAs were induced (Figure 3A). Immunoblot analysis of EMMPRIN expression revealed the presence of three major immunoreactive fragments of 25, 37, and 50 kDa in wild-type resting mice, corresponding to different levels of EMMPRIN glycosylation.[24] The association between NO and EMMPRIN during AAA was evaluated in wild-type and iNOS null mouse aortas. As result of elastase infusion, a significant increase of EMMPRIN was detected in wild-type mice, whereas in iNOS null mice, we could barely detect the two major high molecular fragments of EMMPRIN, both in resting and in elastase-infused aortas (Figure 3B). By contrast, no differences were detected when AAA were induced in wild-type 12-week-old mice (data not shown), in which iNOS levels were significantly lower respect to aged animals in response to elastase infusion (Figure 1C). However, exogenous administration of the NO donor Spermidine-nonoate in young mice after infusion of elastase by i.p. injection reported a substantial increase of EMMPRIN levels in the abdominal aortas (Supplemental Figure S4A, see *http://ajp.amjpathol.org*).

NO Regulates the Expression of EMMPRIN during AAA

To further explore the effect of NO on EMMPRIN expression, we evaluated the progression of AAA in aged iNOS null mice, in which NO was daily administered by i.p. injection of the NO donor Spermidine-nonoate over 15 days. We found that in iNOS null mice, the administration of NO induced a significant increase of aortic dilatation (Figure 3C), collagen, and elastin fibers degradation, as detected by Masson and Verhoeff-van Gieson staining, increased protein nitration, as detected by immunofluorescence with anti-nitro-tyrosine antibody, and increased EMMPRIN and MMP-13 levels, as detected with specific antibodies (Figure 3D) over mice treated with the drug control of the NO donor (Spermidine), resembling the inflammatory response to the vascular injury elicited in wild-type mice. Additional markers of inflammation were also evaluated in these animals (Supplemental Figure S5, see *http://ajp.amjpathol.org*). By contrast, inhibition of iNOS by daily i.p. injection with the pharmacological inhibitor 1400 W preserved collagen and elastin fibers, and protein nitration was reduced (Figure 3E), as well as expression of EMMPRIN and MMP-13 (Figure 3F).

Overexpression of EMMPRIN Induces MMP-13 Accumulation at the Extracellular Space

EMMPRIN was found to induce activation of different MMPs, yet no data regarding MMP-13 was reported so far. The results presented above lead us to investigate the possible association between EMMPRIN and MMP-13, and taking into account that EMMPRIN was located in endothelial cells (Figure 3A), we overexpressed FLAG-tagged EMMPRIN in vascular aortic endothelial cells isolated from mouse aortas (Supplemental Figure S4B, see *http://ajp.amjpathol.org*). In cells expressing ectopic-EMMPRIN, MMP-13 expression was down-regulated as detected by immunoblot from cell lysates (Figure 4A, MMP-13 lysate panel). However, immunoblot analysis with anti-FLAG and anti-MMP-13 antibodies from cultured media revealed that FLAG-EMMPRIN induced MMP-13 secretion (Figure 4A, MMP-13 culture media), suggesting for the first time that EMMPRIN may regulate MMP-13 activity in vascular endothelium.

Down-Regulation of EMMPRIN Inhibits MMP-13 Expression

To further investigate the association of EMMPRIN and MMP-13, we silenced EMMPRIN in aortic endothelial cells by RNA interference, finding that EMMPRIN does not only induce MMP-13 activity but in addition EMMPRIN regulates MMP-13 expression, since we found that MMP-13 was also down-regulated in these cells (Figure 4B, left panel). In addition, the stimulatory effect of NO on MMP-13 expression was inhibited in small interfering RNA-silenced endothelial cells (Figure 4B, right islet). Taken together, these results point toward EMMPRIN as

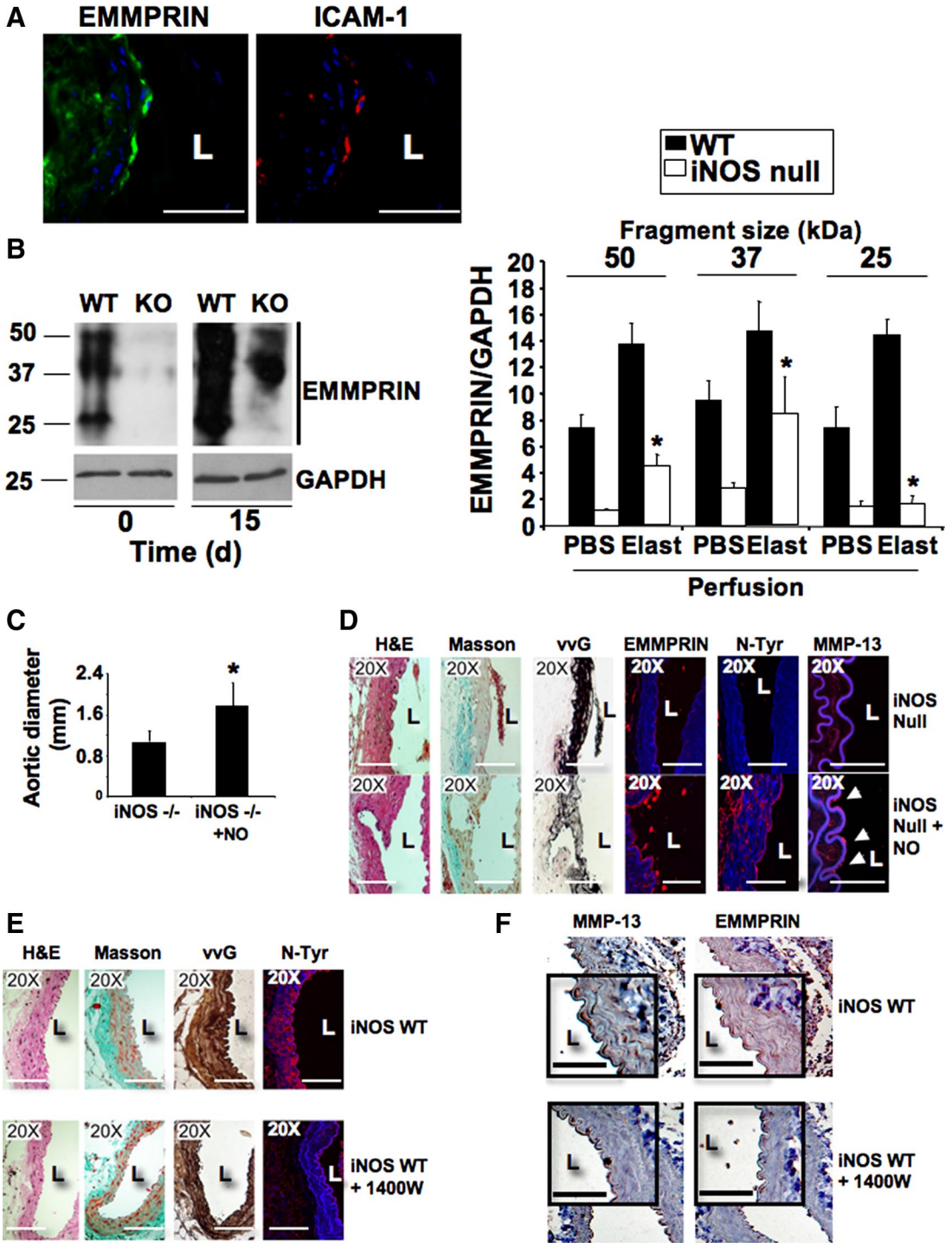

Figure 3. EMMPRIN expression is inhibited in iNOS null mice. **A:** Detection of EMMPRIN (FITC, green) and the endothelial marker ICAM-1 (Cy3, red) by immunohistofluorescence in aortic rings isolated from elastase-infused mice 15 days after surgery. Scale bars, 50 μm. **B:** Immunoblot analysis of EMMPRIN expression in wild-type (WT) and iNOS null mice (knockout (KO)). Three major immunoreactive bands of EMMPRIN were detected, corresponding to different glycosylation levels. GAPDH was also detected for control loading purposes. **Right**, Densitometric analysis of signals detected at time points 0 and 15 after surgery ($n = 3$ mice/time point by triplicate, mean ± SD; $P < 0.05$ wild-type elastase versus iNOS null elastase). **C:** Diameter of iNOS null mouse and iNOS null mouse aortas in which 5 mmol/L Spermidine-nonoate was administered ($iNOS^{-/-}$ + NO), 15 days after elastase infusion (($n = 3$ mice by triplicate, mean ± SD; $^{*}P < 0.05$ versus iNOS null). **D:** Representative micrographs of aortic serial sections of the same mice as in **C**, in which HE, Masson Trichrome, Verhoeff-van Gieson staining, EMMPRIN, protein tyrosine nitration, and MMP-13 expression were detected. **Arrows** point endothelial positive cells ($n = 3$). Scale bars, 50 μm. **E:** Representative micrographs of aortic serial sections isolated from iNOS wild-type mice in which 500 μmol/L 1400W was daily administered, 15 days after elastase infusion, showing HE, Masson Trichrome, Verhoeff-van Gieson staining, and protein tyrosine nitration ($n = 3$ mice/group by tryplicate). Scale bars, 50 μm. **F:** Immunohistochemistry detection of MMP-13 and EMMPRIN in aortic sections of the same mice as in **E**. A detailed selection was highlighted in the open squares. Scale bars, 50 μm.

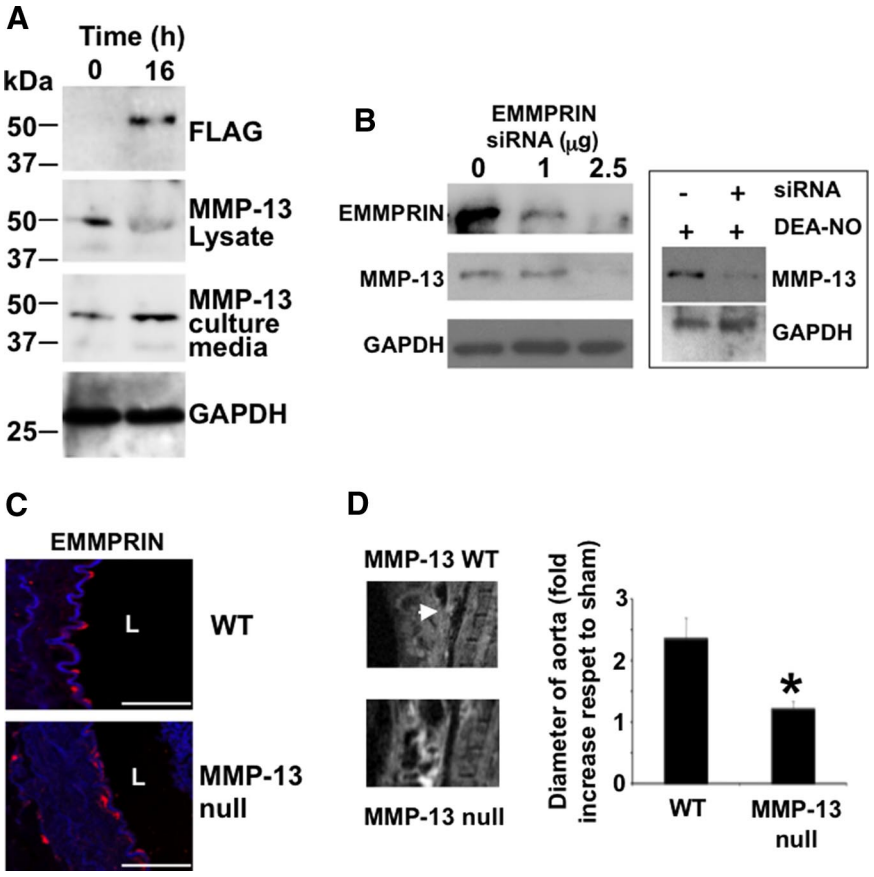

Figure 4. EMMPRIN regulates MMP-13 expression and activity in vascular endothelium. **A:** Immunoblot detection of ectopic FLAG-EMMPRIN, and endogenous MMP-13 in cell lysates and culture medium of FLAG-EMMPRIN expressing murine aortic endothelial cells. GAPDH was also detected for control loading purposes. **B:** Immunoblot detection of ectopic FLAG-EMMPRIN and endogenous MMP-13 in cell lysates and culture medium from murine aortic endothelial cells in which EMMPRIN was silenced. GAPDH was also detected for control loading purposes ($n = 3$ by triplicate). **Right**, Expression of MMP-13 in endothelial cells treated with 100 μmol/L DEA-NO in silenced-EMMPRIN cells. **C:** Detection of EMMPRIN in aortic rings of wild-type and MMP-13 null mice, 15 days after surgery. L: lumen. $n = 3$. Scale bars, 50 μm. **D:** 10 animals/group were either infused with elastase or saline buffer and the aneurysms (**arrow**) were monitored over time by magnetic resonance. **Right**, Graphical representation of aortic dilatation 15 days after surgery respect to sham operated mice ($n = 10$ mice/genotype/assay by triplicate mean ± SD; $^{*}P < 0.05$ versus wild-type).

an upstream regulator of MMP-13 and suggest that NO-mediated EMMPRIN expression may contribute to the progression of AAA through activation of different MMPs, including MMP-13. In support of this concept, we found that after elastase infusion of MMP-13 null mouse aortas, and even when no differences were detected on EMMPRIN expression (Figure 4C), aortic dilatation was significantly reduced in these mice when compared with their wild-type counterparts (Figure 4D).

EMMPRIN, MMP-13, and iNOS Are Expressed in Human AAAs

To evaluate if EMMPRIN and MMP-13 are involved in human aneurysms, we took biopsies from 18 patients subjected to clinical intervention (Supplemental Table 1, see *http://ajp.amjpathol.org*). We found that EMMPRIN and MMP-13 were both expressed in endothelial cells and smooth muscle cells, as detected by immunohistochemistry with specific antibodies. In these samples, we also found iNOS expression (Figure 5A, upper panel), detecting a correlation between iNOS levels and iNOS activity as detected by nitrotyrosine staining (Figure 5B). Control biopsies did show no significant expression of iNOS, MMP-13, or EMMPRIN (Figure 5A, lower panel).

Discussion

Our study has identified a molecular mechanism for the NO-mediated AAA progression, by the induction of the MMP inducer EMMPRIN. In mice and in human aneurysms, iNOS, EMMPRIN, and MMP-13 are expressed, although gene-targeted disruption of iNOS inhibit EMMPRIN and MMP expression in mice. In healthy iNOS null mice, EMMPRIN levels are significantly reduced as compared with their wild-type counterparts, and AAA did not promote significant changes either on expression and glycosylation. The effect of EMMPRIN on MMP-13 expression was found in overexpressing-EMMPRIN-, and in small interfering RNA-EMMPRIN-silenced aortic endothelial cells. The relevance of these findings were further verified in MMP-13 null mice, showing decreased AAA formation when compared with wild-type mice.

The role of iNOS on AAA is documented in animals and humans.[17,25] In general, NO is associated to progression of AAA, in which a correlation between NO-mediated nitrotyrosine modification of proteins and vascular injury was detected.[26] However, downstream signaling pathways elicited by NO are still missing. We propose EMMPRIN as a target of NO leading to conversion of proMMPs into active MMPs in AAA.

Lee et al[17] found that in 12-week-old iNOS null mice, no significant morphological changes respect to wild-

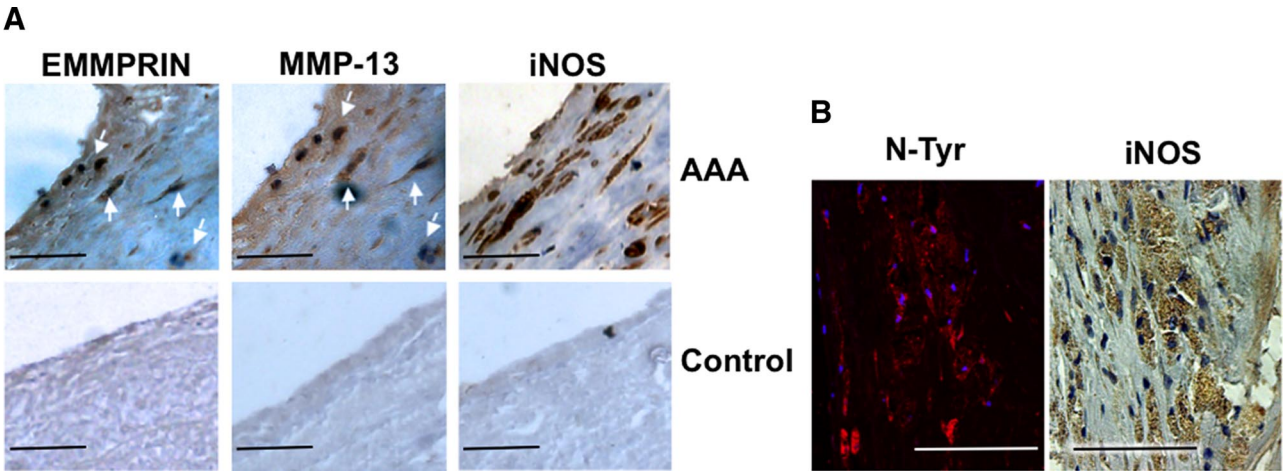

Figure 5. EMMPRIN, MMP-13, iNOS, and nitro-tyrosine detection in human AAA. **A:** EMMPRIN, MMP-13, and iNOS, expression in AAA samples ($n = 18$) (**upper**) or in control aortas ($n = 3$) (**lower**). Serial sections showing colocalization of EMMPRIN and MMP-13 (**arrows**) are depicted. **B:** Aortic serial sections showing immunofluorescence detection of nitrotyrosine by confocal microscopy (**left**, Red-Cy3, DAPI-nuclei), and immunohistochemistry detection of iNOS by using bright field microscopy (**right**). Colocalization of both signals was also detected.

type animals were detected. However, as we mentioned above, we and others found that lack of iNOS protects aged mice during progression of AAA. Even though the authors found extensive protein tyrosine nitration and iNOS expression in wild-type animals, they also state that it appears unlikely that increased aortic wall production of NO and protein nitration are innocuous events. Protein nitration is considered deleterious in patients and mice, not only in AAA, but also during the occurrence of other cardiovascular diseases.[27] AAA is an age-related condition, affecting mostly at people age 60 and older. We performed our study in adult mice (12 weeks) and aged mice (45 to 50 weeks), finding that aged animals show significant differences in AD, and expression of iNOS in response to elastase infusion. In addition, exogenous administration of NO to iNOS null mice induced significant increase of AD, MMP-13 and EMMPRIN expression, whereas pharmacological inhibition of iNOS in wild-type mice induced the opposite. Age-related dysregulation of inflammatory mediators, including the expression of iNOS, is well established, and is the source of age-dependent deleterious effects.[28]

NO and MMPs significantly contribute to the pathogenesis of AAA. However, the implication of NO on MMP regulation in this context was limited to the study of MMP-9, with apparent controversy. In rat AAA, pharmacological inhibition of NOS, or treatment with statins inhibited NO production and MMP-13 expression.[29,30] By contrast, in murine AAA,[31] NO-mediated AAA are not related to MMP-9 activation, as also described here as well. We previously found that NO induces the expression of MMP-13 in aortic endothelial cells.[18] Here, we uncovered for the first time the association of NO and MMP-13 in murine and human aneurysms.

The mechanisms by which NO induces progression of AAA may lie in fact that MMP-13 can cleave a wide variety of extracellular matrix components used by endothelial cells to attach to the vessel wall, including interstitial collagens I and III, as previously reported in human AAA,[3] but in addition, secretion of MMP-13 by endothelial cells may also regulate the initial inflammatory steps by modulating monocyte and leukocyte adhesion and trafficking, as previously reported for MMP-2 and MMP-9.[32] In the context of atherosclerosis, we previously found significant monocyte infiltration in endothelial nitric oxide synthase (NOS3)/apoE double null mice when compared apoE animals.[20] However, iNOS null mice did not show differences in immune cell infiltration during AAA, when compared with their wild-type counterparts.

EMMPRIN is an immunoglobulin mediator present in atherosclerosis, hypertension, myocardial infarction, and stroke,[7,15,21–24] and we found that EMMPRIN is also involved in the progression of aneurysms. Data regarding upstream regulation of EMMPRIN in cardiovascular disease are limited to Chlamidia hsp 60,[14] or PPAR-α and -γ[33] in cultured monocytes. Here we provide *in vivo* evidence pointing EMMPRIN as a downstream signaling effector in the NO-mediated MMP expression during aneurysmal progression.

EMMPRIN-mediated induction of MMPs is dependent on glycosylation. EMMPRIN is associated to caveolin-1 in multiple cell types, including endothelial cells and smooth muscle cells, and caveolin-1 inhibit EMMPRIN glycosylation.[34] Hence, signals triggering EMMPRIN release from caveolin-1, may therefore cause conversion of pro-MMP to active MMP. The membrane type metalloproteinase MT1-MMP,[35] is activated by EMMPRIN on monocytes and smooth muscle cells,[7] and MT1-MMP is found to induce activation of MMP-13.[36] MT1-MMP and MMP-13 are also found associated to caveolin-1, and NO induces MMP-13 expression, MMP-13 activation,[18] and disrupts the complex MMP-13/caveolin-1 in aortic endothelial cells.[16]

NO may induce MMP-13 at different levels. NO may promote dissociation of EMMPRIN from caveolin-1, increasing EMMPRIN expression, NO may elicit dissociation of MT1-MMP from caveolin-1, but in addition, we cannot exclude a direct effect of NO on MMP-13 activation by inducing direct posttranslational modification as it

does with other MMPs,[37–39] including MMP-13 in the context of wound healing.[19]

This study shows for the first time the involvement of EMMPRIN in murine and human AAA, and the association with MMP-13 in the NO-mediated AAA. The regulation of NO and EMMPRIN glycosylation, may be crucial for controlling elastic tissue degradation in AAA.

Acknowledgments

We thank Dr. Encarnación Fernández-Valle for assistant with magnetic resonance imaging acquisition data, Dr. Carlos López Otín and Dr. Stephen Krane for kindly donation of MMP-13 null mice, Dr. Francisco Sánchez Madrid, for donation of antibody to human EMMPRIN, Drs. Jesus Egido, Jose Luis Martin-Ventura, and Jean Baptiste Michel for donation of aortic tissue, and Dr. Valentín Fuster for helpful advice and suggestions.

References

1. Baril DT, Jacobs TS, Marin ML: Surgery insight: advances in endovascular repair of abdominal aortic aneurysms. Nat Clin Pract Cardiovasc Med 2007, 4:206–213
2. Ernst CB: Abdominal aortic aneurysm. N Engl J Med 1993, 328: 1167–1172
3. Mao D, Lee JK, VanVickle SJ, Thompson RW: Expression of collagenase-3 (MMP-13) in human abdominal aortic aneurysms and vascular smooth muscle cells in culture. Biochem Biophys Res Commun 1999, 261:904–910
4. Abdul-Hussien H, Soekhoe RG, Weber E, von der Thusen JH, Kleemann R, Mulder A, van Bockel JH, Hanemaaijer R, Lindeman JH: Collagen degradation in the abdominal aneurysm: a conspiracy of matrix metalloproteinase and cysteine collagenases. Am J Pathol 2007, 170:809–817
5. Longo GM, Xiong W, Greiner TC, Zhao Y, Fiotti N, Baxter BT: Matrix metalloproteinases 2 and 9 work in concert to produce aortic aneurysms. J Clin Invest 2002, 110:625–632
6. Eagleton MJ, Ballard N, Lynch E, Srivastava SD, Upchurch GR Jr, Stanley JC: Early increased MT1-MMP expression and late MMP-2 and MMP-9 activity during Angiotensin II induced aneurysm formation. J Surg Res 2006, 135:345–351
7. Schmidt R, Bultmann A, Ungerer M, Joghetaei N, Bulbul O, Thieme S, Chavakis T, Toole BP, Gawaz M, Schomig A, May AE: Extracellular matrix metalloproteinase inducer regulates matrix metalloproteinase activity in cardiovascular cells: implications in acute myocardial infarction. Circulation 2006, 113:834–841
8. Caudroy S, Polette M, Nawrocki-Raby B, Cao J, Toole BP, Zucker S, Birembaut P: EMMPRIN-mediated MMP regulation in tumor and endothelial cells. Clin Exp Metastasis 2002, 19:697–702
9. Caudroy S, Polette M, Tournier JM, Burlet H, Toole B, Zucker S, Birembaut P: Expression of the extracellular matrix metalloproteinase inducer (EMMPRIN) and the matrix metalloproteinase-2 in bronchopulmonary and breast lesions. J Histochem Cytochem 1999, 47:1575–1580
10. Haseneen NA, Vaday GG, Zucker S, Foda HD: Mechanical stretch induces MMP-2 release and activation in lung endothelium: role of EMMPRIN. Am J Physiol Lung Cell Mol Physiol 2003, 284:L541–L547
11. Kanekura T, Chen X, Kanzaki T: Basigin (CD147) is expressed on melanoma cells and induces tumor cell invasion by stimulating production of matrix metalloproteinases by fibroblasts. Int J Cancer 2002, 99:520–528
12. Norgauer J, Hildenbrand T, Idzko M, Panther E, Bandemir E, Hartmann M, Vanscheidt W, Herouy Y: Elevated expression of extracellular matrix metalloproteinase inducer (CD147) and membrane-type matrix metalloproteinases in venous leg ulcers. Br J Dermatol 2002, 147:1180–1186
13. Sameshima T, Nabeshima K, Toole BP, Yokogami K, Okada Y, Goya T, Koono M, Wakisaka S: Glioma cell extracellular matrix metalloproteinase inducer (EMMPRIN) (CD147) stimulates production of membrane-type matrix metalloproteinases and activated gelatinase A in cocultures with brain-derived fibroblasts. Cancer Lett 2000, 157:177–184
14. Schmidt R, Redecke V, Breitfeld Y, Wantia N, Miethke T, Massberg S, Fischel S, Neumann FJ, Schomig A, May AE: EMMPRIN (CD 147) is a central activator of extracellular matrix degradation by Chlamydia pneumoniae-infected monocytes: implications for plaque rupture. Thromb Haemost 2006, 95:151–158
15. Yoon YW, Kwon HM, Hwang KC, Choi EY, Hong BK, Kim D, Kim HS, Cho SH, Song KS, Sangiorgi G: Upstream regulation of matrix metalloproteinase by EMMPRIN: extracellular matrix metalloproteinase inducer in advanced atherosclerotic plaque. Atherosclerosis 2005, 180:37–44
16. Lopez-Rivera E, Lizarbe TR, Martinez-Moreno M, Lopez-Novoa JM, Rodriguez-Barbero A, Rodrigo J, Fernandez AP, Alvarez-Barrientos A, Lamas S, Zaragoza C: Matrix metalloproteinase 13 mediates nitric oxide activation of endothelial cell migration. Proc Natl Acad Sci USA 2005, 102:3685–3690
17. Lee JK, Borhani M, Ennis TL, Upchurch GR Jr, Thompson RW: Experimental abdominal aortic aneurysms in mice lacking expression of inducible nitric oxide synthase. Arterioscler Thromb Vasc Biol 2001, 21:1393–1401
18. Zaragoza C, Balbin M, Lopez-Otin C, Lamas S: Nitric oxide regulates matrix metalloprotease-13 expression and activity in endothelium. Kidney Int 2002, 61:804–808
19. Lizarbe TR, Garcia-Rama C, Tarin C, Saura M, Calvo E, Lopez JA, Lopez-Otin C, Folgueras AR, Lamas S, Zaragoza C: Nitric oxide elicits functional MMP-13 protein tyrosine nitration during wound repair. FASEB J 2008, 22:3207–3215
20. Tarin C, Gomez M, Calvo E, Lopez JM, Zaragoza C. Endothelial nitric oxide deficiency reduces MMP-13-mediated cleavage of ICAM-1 in vascular endothelium: a role in atherosclerosis. Arterioscler Thromb Vasc Biol 2009 29:27–32
21. Choi EY, Kim D, Hong BK, Kwon HM, Song YG, Byun KH, Park HY, Whang KC, Kim HS: Up-regulation of extracellular matrix metalloproteinase inducer (EMMPRIN) and gelatinases in human atherosclerosis infected with Chlamydia pneumoniae: the potential role of Chlamydia pneumoniae infection in the progression of atherosclerosis. Exp Mol Med 2002, 34:391–400
22. Sidhu SS, Mengistab AT, Tauscher AN, LaVail J, Basbaum C: The microvesicle as a vehicle for EMMPRIN in tumor-stromal interactions. Oncogene 2004, 23:956–963
23. Ergul A, Portik-Dobos V, Hutchinson J, Franco J, Anstadt MP: Down-regulation of vascular matrix metalloproteinase inducer and activator proteins in hypertensive patients. Am J Hypertens 2004, 17:775–782
24. Sluijter JP, Pulskens WP, Schoneveld AH, Velema E, Strijder CF, Moll F, de Vries JP, Verheijen J, Hanemaaijer R, de Kleijn DP, Pasterkamp G: Matrix metalloproteinase 2 is associated with stable and matrix metalloproteinases 8 and 9 with vulnerable carotid atherosclerotic lesions: a study in human endarterectomy specimen pointing to a role for different extracellular matrix metalloproteinase inducer glycosylation forms. Stroke 2006, 37:235–239
25. Johanning JM, Franklin DP, Han DC, Carey DJ, Elmore JR: Inhibition of inducible nitric oxide synthase limits nitric oxide production and experimental aneurysm expansion. J Vasc Surg 2001, 33:579–586
26. Zhang J, Schmidt J, Ryschich E, Mueller-Schilling M, Schumacher H, Allenberg JR: Inducible nitric oxide synthase is present in human abdominal aortic aneurysm and promotes oxidative vascular injury. J Vasc Surg 2003, 38:360–367
27. Peluffo G, Radi R: Biochemistry of protein tyrosine nitration in cardiovascular pathology. Cardiovasc Res 2007, 75:291–302
28. Chung HY, Sung B, Jung KJ, Zou Y, Yu BP: The molecular inflammatory process in aging. Antioxid Redox Signal 2006, 8:572–581
29. Johanning JM, Armstrong PJ, Franklin DP, Han DC, Carey DJ, Elmore JR: Nitric oxide in experimental aneurysm formation: early events and consequences of nitric oxide inhibition. Ann Vasc Surg 2002, 16:65–72
30. Kalyanasundaram A, Elmore JR, Manazer JR, Golden A, Franklin DP, Galt SW, Zakhary EM, Carey DJ: Simvastatin suppresses experimental aortic aneurysm expansion. J Vasc Surg 2006, 43:117–124
31. Armstrong PJ, Franklin DP, Carey DJ, Elmore JR: Suppression of experimental aortic aneurysms: comparison of inducible nitric oxide

synthase and cyclooxygenase inhibitors. Ann Vasc Surg 2005, 19:248–257
32. Reichel CA, Rehberg M, Bihari P, Moser CM, Linder S, Khandoga A, Krombach F: Gelatinases mediate neutrophil recruitment in vivo: evidence for stimulus specificity and a critical role in collagen IV remodeling. J Leukoc Biol 2008, 83:864–874
33. Zhang J, Ge H, Wang C, Guo TB, He Q, Shao Q, Fan Y: Inhibitory effect of PPAR on the expression of EMMPRIN in macrophages and foam cells. Int J Cardiol 2007, 117:373–380
34. Tang W, Hemler ME: Caveolin-1 regulates matrix metalloproteinases-1 induction and CD147/EMMPRIN cell surface clustering. J Biol Chem 2004, 279:11112–11118
35. Galvez BG, Matias-Roman S, Yanez-Mo M, Vicente-Manzanares M, Sanchez-Madrid F, Arroyo AG: Caveolae are a novel pathway for membrane-type 1 matrix metalloproteinase traffic in human endothelial cells. Mol Biol Cell 2004, 15:678–687
36. Knauper V, Will H, Lopez-Otin C, Smith B, Atkinson SJ, Stanton H, Hembry RM, Murphy G: Cellular mechanisms for human procollagenase-3 (MMP-13) activation: evidence that MT1-MMP (MMP-14) and gelatinase a (MMP-2) are able to generate active enzyme. J Biol Chem 1996, 271:17124–17131
37. Gu Z, Kaul M, Yan B, Kridel SJ, Cui J, Strongin A, Smith JW, Liddington RC, Lipton SA: S-nitrosylation of matrix metalloproteinases: signaling pathway to neuronal cell death. Science 2002, 297:1186–1190
38. Rajagopalan S, Meng XP, Ramasamy S, Harrison DG, Galis ZS: Reactive oxygen species produced by macrophage-derived foam cells regulate the activity of vascular matrix metalloproteinases in vitro: implications for atherosclerotic plaque stability. J Clin Invest 1996, 98:2572–2579
39. Brown DJ, Lin B, Chwa M, Atilano SR, Kim DW, Kenney MC: Elements of the nitric oxide pathway can degrade TIMP-1 and increase gelatinase activity. Mol Vis 2004, 10:281–288